Organic Geochemistry 164 (2022) 104347

Contents lists available at ScienceDirect

Organic Geochemistry

journal homepage: www.elsevier.com/locate/orggeochem

Soil pH and aridity influence distributions of branched tetraether lipids in grassland soils along an aridity transect

Jingjing Guo [a,*], Tian Ma [b,c], Nana Liu [d], Xinying Zhang [b,e], Huifeng Hu [b], Wenhong Ma [f], Zhiheng Wang [g], Xiaojuan Feng [b,e], Francien Peterse [a]

[a] Department of Earth Sciences, Utrecht University, 3584 CB Utrecht, the Netherlands
[b] State Key Laboratory of Vegetation and Environmental Change, Institute of Botany, Chinese Academy of Sciences, 100093 Beijing, China
[c] State Key Laboratory of Grassland Agro-Ecosystems, College of Pastoral Agriculture Science and Technology, Lanzhou University, 730000 Lanzhou, China
[d] State Key Laboratory of Mycology, Institute of Microbiology, Chinese Academy of Sciences, 100190 Beijing, China
[e] College of Resources and Environment, University of Chinese Academy of Sciences, 100049 Beijing, China
[f] College of Ecology and Environment, Inner Mongolia University, 010021 Hohhot, China
[g] Institute of Ecology and Key Laboratory for Earth Surface Processes of the Ministry of Education, College of Urban and Environmental Sciences, Peking University, 100871 Beijing, China

ARTICLE INFO

Associate Editor — **Johan Weijers**

Keywords:
brGDGTs
Soil pH
Aridity
Acidobacteria
Verrucomicrobia
Actinobacteria
Environmental proxy

ABSTRACT

Branched glycerol dialkyl glycerol tetraethers (brGDGTs) are membrane lipids of certain soil bacteria, and their relative distributions are used as a proxy for air temperature and soil pH. While temperature is recorded by the degree of methylation, soil pH is reflected by the amount of internal cyclization and the relative abundance of 6-methyl isomers. Since the exact producers of brGDGTs remain enigmatic, the mechanisms underlying their empirical relationships with temperature and soil pH, and thus the reliability of brGDGT-based paleorecords, are not well understood, especially in arid regions where mean annual precipitation (MAP) is less than 500 mm. Here, we evaluate the influence of soil pH and aridity on brGDGT distributions in grassland soils along an aridity transect (MAP = 173–415 mm) in Inner Mongolia. While the absolute and fractional abundance of 6-methyl brGDGTs increases with increasing soil pH and aridity, following the trend in the global surface soil calibration dataset, the degree of cyclization does not. This indicates that in arid regions, soil pH reconstructions based on the relative contribution of 6-methyl brGDGTs are likely more reliable than those based on the degree of cyclization. Furthermore, 5- and 6-methyl brGDGTs respond differently to aridity, supporting prior suggestions that the distribution of brGDGTs could be the result of changes in bacterial community composition instead of the direct physiological alteration of molecular structures by the source organisms. Analysis of the bacterial community composition in the same soil transect indicates that the relative abundance of Acidobacteria, the phylum hosting potential brGDGT source-organisms, shows a poor relationship with aridity. Instead, Verrucomicrobia ($r^2 = 0.70$, $p < 0.01$), and its subclass Spartobacteria ($r^2 = 0.70$, $p < 0.01$) in particular, show a significant negative correlation with aridity, resembling that of 5-methyl brGDGTs. Similarly, Actinobacteria are positively correlated with aridity ($r^2 = 0.59$, $p < 0.01$), following the same trend as that of 6-methyl brGDGTs. The ability of certain cultures of Verrucomicrobia and Actinobacteria to produce *iso*-$C_{15:0}$ fatty acids that could serve as building blocks for brGDGTs hints that Verrucomicrobia and Actinobacteria could possibly produce brGDGTs in arid soils.

1. Introduction

Branched glycerol dialkyl glycerol tetraethers (brGDGTs) are a suite of membrane-spanning lipids synthesized by heterotrophic bacteria that thrive in soils, peats, the water column of lakes and rivers, as well as lacustrine and marine sediments (Schouten et al., 2013, and references therein). BrGDGTs can contain 0–2 cyclopentane moieties following internal cyclization, as well as 4–6 methyl branches attached to their alkyl chains, where the outer methyl branch can be attached to either the C-5, C-6, or C-7 position (Sinninghe Damsté et al., 2000; Weijers

* Corresponding author.
E-mail address: j.guo@uu.nl (J. Guo).

https://doi.org/10.1016/j.orggeochem.2021.104347
Received 16 September 2021; Received in revised form 22 November 2021; Accepted 22 November 2021
Available online 3 December 2021

et al., 2006; De Jonge et al., 2013; Ding et al., 2016). Based on their relative distribution in a global collection of surface soils, the degree of methylation of 5-methyl brGDGTs (quantified in the MBT'$_{5Me}$) has been linked to mean annual air temperature (MAT), whereas the cyclization of branched tetraethers and the relative abundance of 6-methyl brGDGTs are related to soil pH and quantified in the CBT' and the isomer ratio IR (Weijers et al., 2007; Peterse et al., 2012; De Jonge et al., 2014a,b). Although these empirical relationships allow the use of brGDGTs as proxies for paleoclimate reconstructions, the temperature and pH estimates based on these transfer functions are still associated with a large uncertainty (4.8 °C for temperature and 0.5 for pH, respectively; De Jonge et al., 2014a).

This uncertainty can in part be attributed to our incomplete understanding of the exact mechanism underlying the response of brGDGTs to changes in temperature and soil pH, as their producers are still largely unknown. It was initially suggested that brGDGT-producers would alter the molecular structure of their membrane to obtain optimal membrane fluidity and permeability under different temperature and soil pH conditions (Weijers et al., 2007). Although this scenario was recently supported by molecular dynamics simulations of brGDGTs (Naafs et al., 2021), changes in brGDGT distributions have also been proposed to indirectly result from shifts in the composition of soil bacterial communities (i.e., brGDGT-producers) under different environmental conditions (Sinninghe Damsté et al., 2018). In fact, a study on a set of geothermally warmed soils showed that the brGDGT distribution only changes when soil temperature passes a threshold of 14 °C, coinciding with an abrupt shift in the bacterial community (De Jonge et al., 2019). Interestingly, brGDGTs in these geothermally heated soils showed a different temperature dependency below and above this threshold, suggesting that brGDGT distributions more likely reflect an indirect (i.e., bacterial community composition) rather than direct (i.e., membrane adaptation) response to environmental change (De Jonge et al., 2019).

Similar distribution patterns of brGDGTs and Acidobacteria 16S rRNA genes in a Swedish peat profile suggested that this phylum may host the producers of these compounds (Weijers et al., 2009). This was confirmed by the detection of brGDGT-Ia in a culture of Acidobacteria subdivision (SD) 1, as well as the presence of 13,16-dimethyl octacosanedioic acid (*iso*-diabolic acid), a presumed brGDGT precursor lipid in strains from SDs 1, 3, 4, and 6 (Sinninghe Damsté et al., 2011, 2014, 2018). In addition, proposed building blocks of 5-methyl brGDGTs, i.e., a mono-glycerol ether derivative of *iso*-diabolic acid, are so far exclusively detected in SD 4 species, while the strains of SDs 1, 3 and 6 produce 6-methyl *iso*-diabolic acids. Although the contribution of 6-methyl *iso*-diabolic acids is low for some strains of SDs 1 and 3, this implies that 5- and 6-methyl brGDGTs are likely produced by different species (Sinninghe Damsté et al., 2018). Regardless, a biological source outside the phylum of Acidobacteria cannot be excluded. For example, the gene cluster involved in the biosynthesis of ether lipids is also present within the δ-proteobacteria (Sinninghe Damsté et al., 2018), and hence more insight into their producers is needed to verify the response of brGDGTs to temperature and pH in controlled culture experiments.

Another source of uncertainty regarding brGDGT-based proxies is related to confounding factors that, next to temperature and soil pH, also exert an influence on brGDGT distributions. For example, soil moisture has been suggested to influence brGDGT distributions, especially in arid soils that annually receive < 500 mm precipitation and do not experience a pronounced season of rainfall (Peterse et al., 2012; Dirghangi et al., 2013; Menges et al., 2014; Wang et al., 2014; Dang et al., 2016). Indeed, brGDGTs in arid soils do not accurately record actual MAT and show large deviations from the global surface soil calibration dataset, which has led to the development of regional calibrations to reconstruct temperature in arid regions such as the Chinese Loess Plateau (Yang et al., 2014) or Central Asia (Chen et al., 2021). In soils along a soil moisture content gradient (0–61%) around Qinghai Lake, soil moisture availability appeared to impact the degree of methylation of 6-methyl brGDGTs (MBT'$_{6Me}$), while 5-methyl brGDGTs in the same soils primarily responded to temperature (Dang et al., 2016). Based on this finding, Naafs et al. (2017) suggested to exclude all soils with a high relative abundance of 6-methyl brGDGTs (i.e., IR > 0.5) from global temperature calibrations to reduce uncertainties. However, brGDGTs in soils along several elevation transects in the Himalayas faithfully reflected the adiabatic cooling of air, whereas the majority of the samples had an IR > 0.5 (van der Veen et al., 2020). De Jonge et al. (2014a), however, found that removing the influence of 6-methyl brGDGTs from the temperature calibration indeed could resolve the observed offset in arid soils. Nevertheless, the most recent calibration based on an expanded global soil dataset found that excluding soils with IR > 0.5 did not improve the relationship between brGDGTs and MAT and argued for keeping these soils in the global dataset (Dearing Crampton-Flood et al., 2020).

Earlier, Xie et al. (2012) noticed that the global, negative relationship between the initial CBT and soil pH abruptly changed to a positive relationship in arid soils with pH > 7.5. However, this observation was based on a dataset where 5- and 6-methyl brGDGT isomers were not separated, and the CBT thus includes both the degree of cyclization (represented by brGDGT-IIb and brGDGT-IIb') as well as the isomer ratio (represented by brGDGT-IIb'). Separation of the isomers indicates that a CBT purely based on 5-methyl brGDGTs (CBT$_{5Me}$) still results in an underestimation of soil pH in high pH arid soils, but that the redefined CBT', which includes both 6-methyl brGDGTs as well as brGDGTs with cyclopentane moieties, resolves this issue (see respective Figs. 9a and 10a in De Jonge et al., 2014a). Nevertheless, these distinct trends with pH suggests that 5- and 6-methyl brGDGTs and/or brGDGTs with and without cyclization(s) have a different pH dependency in arid soils.

To further investigate the behavior of brGDGTs in arid soils, we here target temperate grassland surface soils along an aridity gradient (MAP = 173–415 mm) in Inner Mongolia, northern China. Grasslands in this arid and semiarid region have a low moisture availability with neutral-to-alkaline soils, providing an ideal platform to investigate brGDGT distributions in moisture-limited environments, which are currently underrepresented in the global soil dataset. We base our analysis on previously published datasets of brGDGTs (Zhang et al., 2020) and 16S rRNA sequencing of soil bacterial communities in the same soils (Liu et al., 2019) to assess potential producers of brGDGTs in these semiarid grasslands, as well as the environmental parameters that control their distribution.

2. Material and methods

2.1. Study site and sampling

A detailed overview of the study area and sampling sites is given by Liu et al. (2019) and Zhang et al. (2020). Briefly, 32 surface soils (0–10 cm) were collected as composite samples from the center and each corner of a 10 m × 10 m square plot at each site along an ~1500 km-long grassland transect in Inner Mongolia, northern China, in the summer of 2015 (Fig. 1a). All soils were cooled upon sampling and stored at −80 °C after transport to the laboratory. Along the transect, mean annual temperature (MAT) decreases from 7.6 °C in the southwest to −2.1 °C in the northeast, while mean annual precipitation (MAP) shows the opposite trend and increases from 173 to 415 mm ($r^2 = 0.55$, $p < 0.01$; Fig. 1b). This translates into an aridity index (AI; the ratio of MAP to potential evapotranspiration) of 0.18–0.56, where a low AI reflects arid conditions. Soils were classified as Chernozems, Kastanozems and Calcisols (IUSS Working Group WRB, 2015) with pH decreasing from 9.9 in the southwest to 7.7 in the northeast, negatively relating to AI ($r^2 = 0.43$, $p < 0.01$; Fig. 1c). The soil organic carbon (SOC) content ranges from 0.4% to 4.7% and decreases with increasing aridity and soil pH (Zhang et al., 2020). The vegetation is characterized as desert steppe in the southwest, changing to typical steppe and subsequently meadow steppe towards the northeast (Fig. 1a).

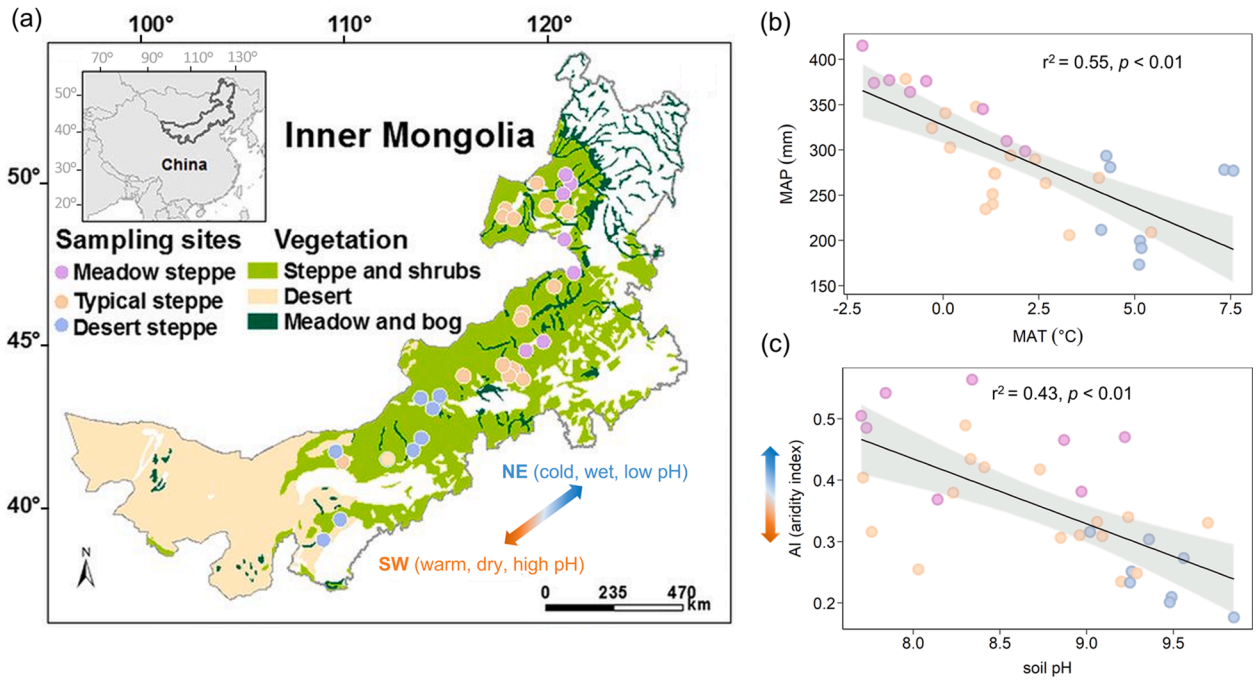

Fig. 1. (a) Spatial distribution of sampling sites and vegetation type across the temperate grasslands in Inner Mongolia, adjusted from Liu et al. (2019). Scatter plots of (b) the mean annual temperature (MAT) versus mean annual precipitation (MAP), and (c) soil pH versus aridity along the Inner Mongolia soil transect ($n = 32$).

2.2. BrGDGT extraction and analysis

BrGDGTs were extracted from 6–7 g freeze-dried and homogenized soil using a modified Bligh-Dyer method (Bligh and Dyer, 1959) at the Institute of Botany, Chinese Academy of Sciences in Beijing, as described in detail by Zhang et al. (2020). Concentrations of total brGDGTs have been reported in Zhang et al. (2020) to compare with other microbial biomarkers (such as phospholipid fatty acids and amino sugars), whereas concentrations of individual compounds, relative abundances and brGDGTs-based proxies for MAT and pH are calculated in this study. In short, brGDGTs were extracted ultrasonically (3 ×) with a mixture of dichloromethane (DCM):methanol (MeOH):0.1 M phosphate buffer (2:1:0.8, v/v/v) at pH 7.4 (5 mL g^{-1} soil), after which the phosphate buffer was replaced by trichloroacetic acid (50 mM) and the soil was extracted two more times. All extracts were combined and concentrated using a rotary evaporator, and then passed over a silica gel column, where core lipids were collected using hexane:ethyl acetate (1:1, v/v, 6 mL). A known amount of C_{46} glycerol trialkyl glycerol tetraethers (GTGT) internal standard was added to this fraction (Huguet et al., 2006), which was subsequently re-dissolved in hexane:isopropanol (99:1, v/v), and passed over a 0.45 μm polytetrafluoroethylene (PTFE) filter. The GDGTs were analyzed on an Agilent 1260 Infinity ultra high performance liquid chromatography (UHPLC) coupled to an Agilent 6130 single quadrupole mass spectrometer (MS) with settings according to Hopmans et al. (2016) at Utrecht University. Quantitation was achieved by peak area integration of the $[M+H]^+$ ions in Chemstation software B.04.03.

BrGDGT proxies were calculated according to the equations listed below, in which the roman numerals refer to the molecular structures shown in Supplementary Fig. S1, and the square brackets indicate the fractional abundance of brGDGTs.

The degree of methylation of 5-methyl brGDGTs (MBT'_{5Me}) and 6-methyl brGDGTs (MBT'_{6Me}) was calculated following De Jonge et al. (2014a):

$$MBT'_{5Me} = \frac{[Ia] + [Ib] + [Ic]}{[Ia] + [Ib] + [Ic] + [IIa] + [IIb] + [IIc] + [IIIa]} \quad (1)$$

$$MBT'_{6Me} = \frac{[Ia] + [Ib] + [Ic]}{[Ia] + [Ib] + [Ic] + [IIa'] + [IIb'] + [IIc'] + [IIIa']} \quad (2)$$

The MBT'_{5Me} was translated to mean air temperature using the $BayMBT_0$ model (Dearing Crampton-Flood et al., 2020) with a prior mean of 3 °C (modern mean air temperature of all months > 0 °C) and a prior standard deviation of 15 °C as model input.

The degree of cyclization of brGDGTs is captured by the cyclization of branched tetraethers index (CBT and CBT'; Weijers et al., 2007; De Jonge et al., 2014a), and the weighted average number of cyclopentane moieties (#rings; Sinninghe Damsté, 2016):

$$CBT = -\log\frac{[Ib] + [IIb] + [IIb']}{[Ia] + [IIa] + [IIa']} \quad (3)$$

$$CBT' = \log\frac{[Ic] + [IIa'] + [IIb'] + [IIc'] + [IIIa'] + [IIIb'] + [IIIc']}{[Ia] + [IIa] + [IIIa]} \quad (4)$$

$$\#rings_{tetra} = \frac{[Ib] + 2*[Ic]}{[Ia] + [Ib] + [Ic]} \quad (5)$$

$$\#rings_{penta5Me} = \frac{[IIb] + 2*[IIc]}{[IIa] + [IIb] + [IIc]} \quad (6)$$

$$\#\text{rings}_{\text{penta6Me}} = \frac{[\text{IIb}'] + 2*[\text{IIc}']}{[\text{IIa}'] + [\text{IIb}'] + [\text{IIc}']} \quad (7)$$

The isomer ratio (IR) was calculated according to De Jonge et al. (2014b):

$$\text{IR} = \frac{[\text{IIa}'] + [\text{IIb}'] + [\text{IIc}'] + [\text{IIIa}'] + [\text{IIIb}'] + [\text{IIIc}']}{[\text{IIa}] + [\text{IIa}'] + [\text{IIb}] + [\text{IIb}'] + [\text{IIc}] + [\text{IIc}'] + [\text{IIIa}] + [\text{IIIa}'] + [\text{IIIb}] + [\text{IIIb}'] + [\text{IIIc}] + [\text{IIIc}']} \quad (8)$$

2.3. Microbial community composition

Bacterial DNA was analyzed in the same soils as the brGDGTs using the MoBio PowerSoil DNA isolation Kit (MoBio Laboratories, Carlsbad, CA, USA). A detailed description of the bacterial DNA extraction, amplification and sequencing can be found in Liu et al. (2019). In short, amplification of the V4 region of the 16S rRNA gene was performed with forward primer 515F (5'-GTGCCAGCMGCCGCGGTAA-3') and the reverse primer 806R (5'-GGACTACHVGGGTWTCTAAT-3'), generating around 253-bp fragments. After generating raw DNA sequences from the Illumina HiSeq 2500 platform, they were further processed on the Galaxy pipeline in Metagenomics for Environmental Microbiology at the Research Center for Eco-Environmental Sciences, Chinese Academy of Sciences. After serially processing, operational taxonomic units (OTUs) clustered at a 97% sequence similarity cut-off and corresponding annotation information were obtained for follow-up analyses.

2.4. Statistical analysis and data visualization

The statistical analysis and data visualization were undertaken in R software (version 4.0.5) (R Core Team, 2021). Due to the non-normal distribution of data, Spearman correlation was used and considered significant at a level of $p < 0.05$. Scatter plots were generated with package "ggplot2".

3. Results and discussion

3.1. Response of brGDGT signals to aridity and soil pH

BrGDGTs were present in all soils, although brGDGTs with cyclopentane moieties (i.e., brGDGT-IIIc, -IIIc', -IIIb, -IIIb', -IIc and -IIc') were often below the detection limit. The total amount of all brGDGTs increases from 1.8 μg g^{-1} SOC in the arid southwest to 7.3 μg g^{-1} SOC in the more humid northeast along the transect (Fig. 2). This is in agreement with previous studies showing that brGDGT concentrations are relatively low in arid, high pH soils (Xie et al., 2012; Dang et al., 2016). While the concentrations of individual 5-methyl brGDGTs all negatively correlate with aridity (corresponding with a positive correlation with AI in Fig. 2), the concentration of 6-methyl brGDGT-IIIa' shows the opposite trend, and brGDGT-IIa' and -IIb' do not consistently vary along the transect (Fig. 2). Most soils are dominated by 6-methyl brGDGTs, as reflected by the IR, which varies between 0.54 and 0.98 and shows a

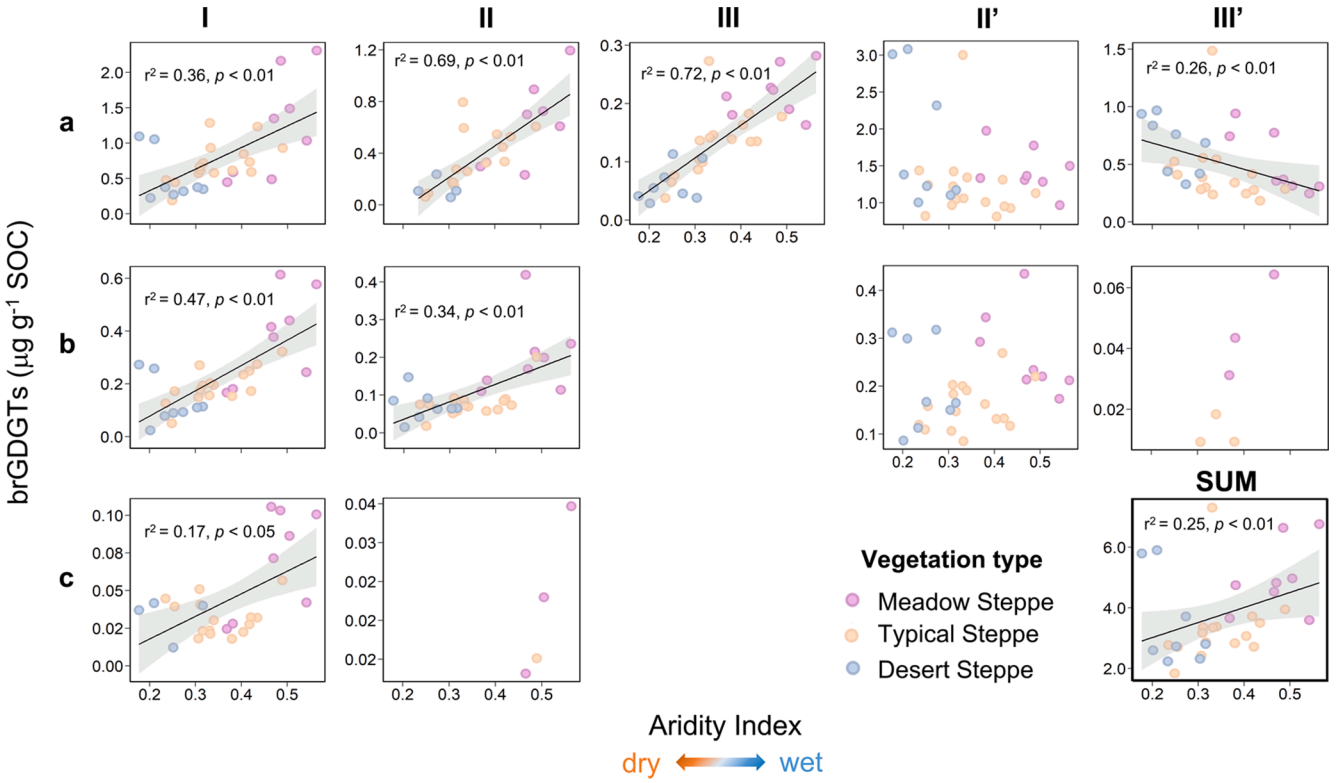

Fig. 2. Spearman's correlation of the concentration of each individual brGDGT compound with the aridity index (AI). The linear regression lines of correlations with $p < 0.05$ are plotted, the 95% confidence intervals are displayed by the gray shaded area. Values below the limit of quantification are not included in the correlation plots. The combination of roman numbers and letters are shown in the supplementary material.

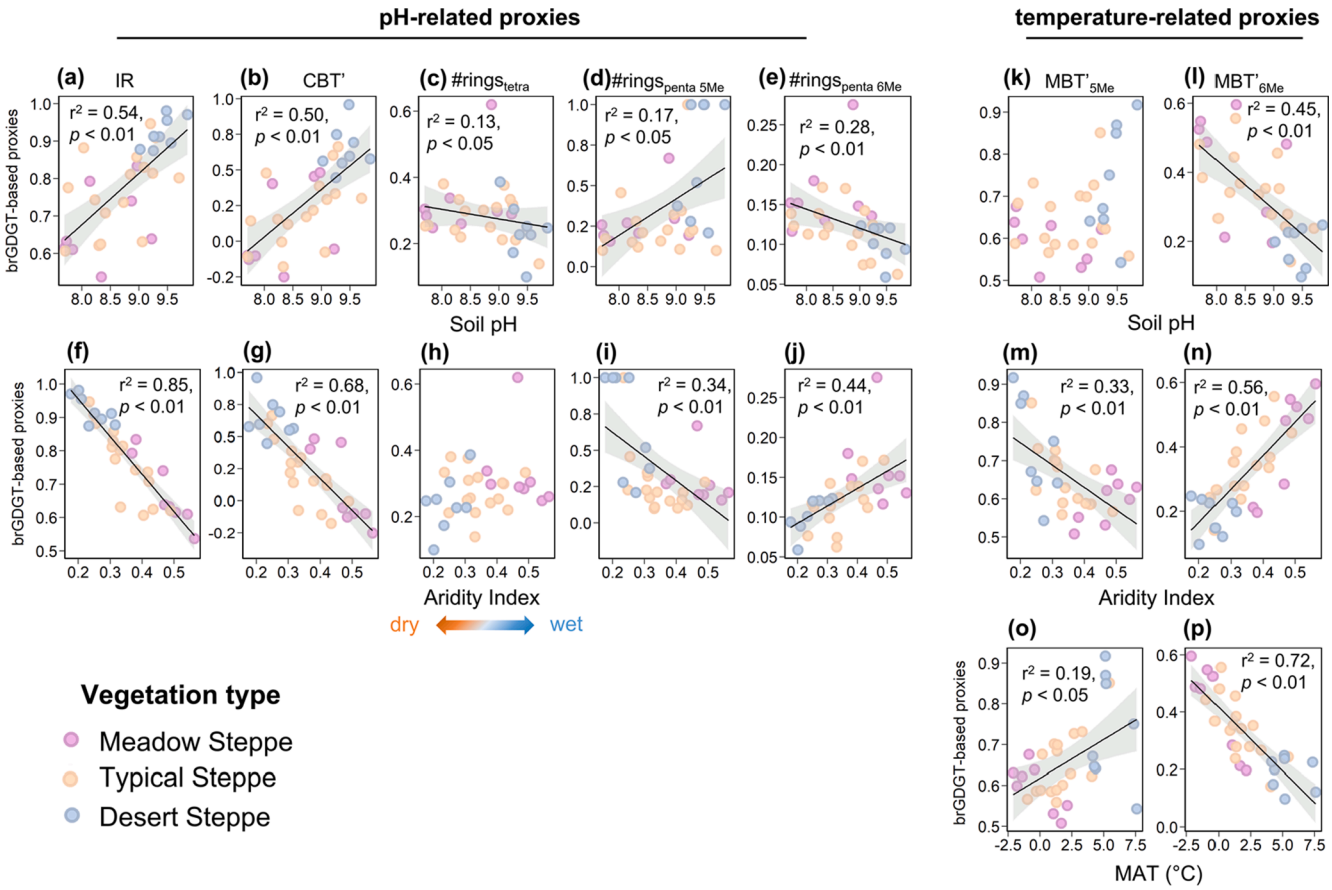

Fig. 3. Spearman's correlation of brGDGT-based pH proxies (a–j) and temperature proxies (k–p) with soil pH, the aridity index (AI), and mean annual air temperature (MAT). The linear regression lines of correlations with $p < 0.05$ are plotted, the 95% confidence intervals are displayed by the gray shaded area.

strong positive relationship with aridity ($r^2 = 0.85$, $p < 0.01$; Fig. 3f). The brGDGT distribution in the soil transect compares well with that in high pH soils from arid Central Asia, which were also characterized by high abundances of brGDGTs-IIIa' and -IIa' as well as a high IR (Chen et al., 2021).

Similar to the global surface soil dataset (De Jonge et al., 2014a), positive relationships of the IR and CBT' with soil pH are also observed in the Inner Mongolia soil transect ($r^2 = 0.54$ and 0.50, $p < 0.01$; Fig. 3a,b). However, the CBT' index not only captures the degree of cyclization, but also the isomer ratio (see Eq. (4)). Since cyclic brGDGTs are either absent, or only occur in relatively low abundances along the transect, the CBT' mostly reflects the relative contribution of 6-methyl brGDGTs in the Inner Mongolia soils. To assess the response of cyclic brGDGTs to soil pH and aridity, we calculate the weighted average number of rings (#rings) for tetra- and pentamethylated 5- and 6-methyl brGDGTs (Fig. 3c–e and h–j). The weighted average number of cyclopentane moieties of tetramethylated brGDGTs (#rings$_{tetra}$, Eq. (5)) only weakly correlates with soil pH ($r^2 = 0.13$, $p < 0.05$; Fig. 3c). This likely results from the negative relationships of both pH and aridity with all tetramethylated brGDGTs in this transect (corresponding with a positive correlation with AI in Fig. 2), whereas brGDGT-Ia has an opposite relationship with pH compared to that of Ib and Ic in the global soil dataset (see Fig. 7 in De Jonge et al., 2014a). A recent study indicated that the concentrations of brGDGTs-Ib and Ic in a pH transect at Craibstone, Scotland, are highest at pH = 7 and then decrease when soil pH further increases (De Jonge et al., 2021). Extrapolating these pH optima to Inner Mongolia can explain the similar trends in concentration for all tetramethylated brGDGTs in soils with pH > 7.5 from the aridity transect, and thus the weak relationship of #rings$_{tetra}$ and soil pH. The correlation of the weighted average number of rings of pentamethylated brGDGTs (#rings$_{penta\ 5Me}$, Eq. (6) and #rings$_{penta\ 6Me}$, Eq. (7)) with soil pH and aridity is slightly stronger than that of the tetramethylated brGDGTs (Fig. 3d, e, i and j), although the #rings values are often only based on two compounds (brGDGT-IIa and -IIb, or -IIa' and -IIb') due to the absence of brGDGTs with two cyclopentane moieties in the majority of the soils, and #rings values only vary within a limited range. Nonetheless, 5- and 6-methyl brGDGTs show opposite behavior along the transect. Specifically, #rings$_{penta\ 5Me}$ shows a positive relationship with soil pH ($r^2 = 0.17$, $p < 0.05$; Fig. 3d) and aridity ($r^2 = 0.34$, $p < 0.01$; corresponding with an opposite correlation with AI in Fig. 3i), whereas #rings$_{penta\ 6Me}$ shows a negative relationship with soil pH and aridity ($r^2 = 0.28$ and 0.44, $p < 0.01$; Fig. 3e,j). Again, this opposite trend likely results from a different pH optimum for the pentamethylated brGDGTs in the Inner Mongolian soils if we assume similar responses to pH as in Craibstone soils, where the pH optimum for brGDGT-IIa lies < 4.5 but at pH = 7 for brGDGT-IIa' (De Jonge et al., 2021). Together with the higher pH optimum for brGDGT-IIb' than for IIb, this results in opposite trends for #rings$_{penta}$ for 5- and 6-methyl brGDGTs at pH > 7.5 (Fig. 3d, e, i and j).

Given the low abundance of cyclic brGDGTs in arid soils as well as the different pH optimum for specific brGDGT compounds, a proxy including cyclic brGDGTs will introduce a bias towards lower soil pH values in arid regions. Thus a transfer function purely based on the relative abundance of 6-methyl brGDGTs, such as previously proposed by Ding et al. (2015), for example, could be used to circumvent the lack of response of cyclic brGDGTs in alkaline soils (pH > 7.5) in high aridity regions. This was supported by a study on a large set of temperate soils from northeast China, where soil pH was more accurately reconstructed using 6-methyl brGDGTs based proxies than those based on the cyclization of brGDGTs (Wang et al., 2016).

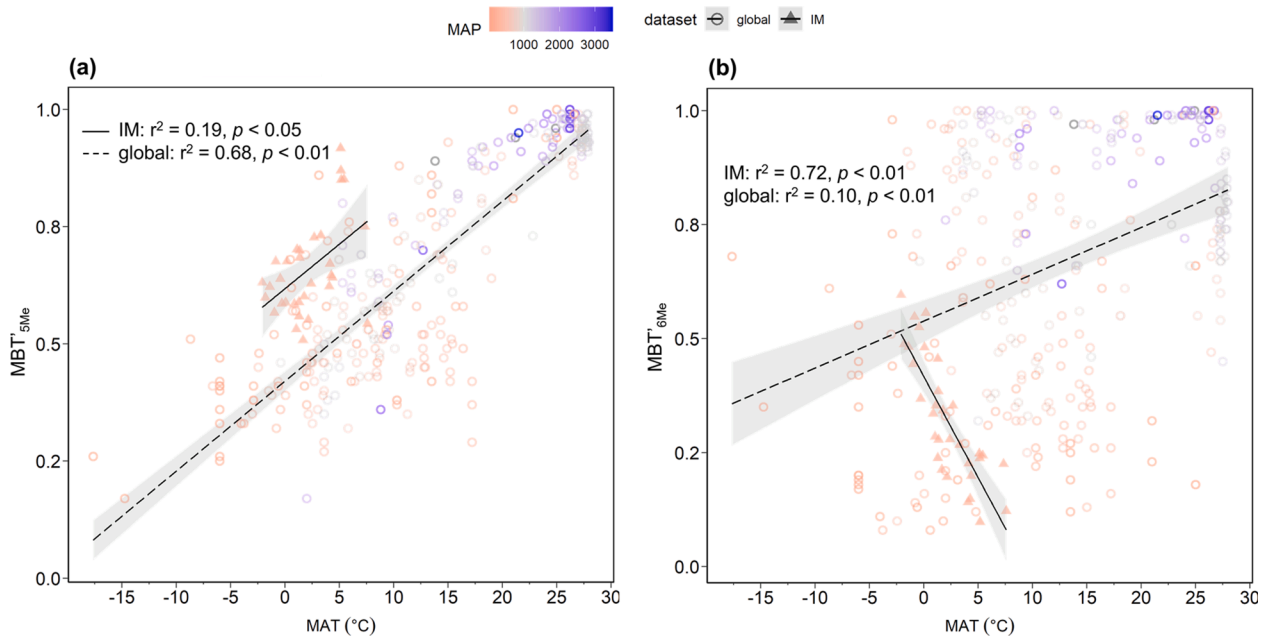

Fig. 4. Spearman's correlation of measured mean annual air temperature (MAT) with (a) methylation of 5-methyl brGDGTs (MBT'$_{5Me}$) and (b) 6-methyl brGDGTs (MBT'$_{6Me}$). The global soils (n = 305, Dearing Crampton-Flood et al., 2020) and Inner Mongolia soil transect (n = 32) are represented by open circles and triangles, respectively. The color gradient indicates the mean annual precipitation (MAP). The linear regression lines of correlations with $p < 0.05$ are plotted with dotted line (global soils) and solid line (Inner Mongolia transect, IM), the 95% confidence intervals are displayed by the gray shaded area.

Likewise, 5- and 6-methyl brGDGTs show opposite trends in their degree of methylation along the transect (temperature-related proxies in Fig. 3k–p), driven by the relationship of brGDGT-IIIa' with aridity (Fig. 2). Although the MBT'$_{5Me}$ (Eq. (1)) shows the expected positive correlation with temperature that is observed in the global soil dataset, the correlation is rather weak ($r^2 = 0.19$, $p < 0.05$; Fig. 4a). In addition, MBT'$_{5Me}$ values are relatively high (0.51–0.92), represented by a substantially higher intercept than that of the global soil dataset (Fig. 4a), and result in an overestimation of actual MAT by up to 18 °C (using BayMBT$_0$; Dearing Crampton-Flood et al., 2020). This indicates that the high pH and aridity in the Inner Mongolia transect influence the general temperature response of 5-methyl brGDGTs. In fact, MBT'$_{5Me}$ correlates best with aridity, where stronger aridity corresponds with more methylations ($r^2 = 0.33$, $p < 0.01$; Fig. 3m). This relationship is opposite to that of MBT'$_{5Me}$ along a soil moisture gradient around Lake Qinghai (Dang et al., 2016), which is a likely result of high soil pH along the Inner Mongolian transect.

Interestingly, the relationships with aridity and temperature along the transect are best captured by MBT'$_{6Me}$ (Fig. 3n and p), although the temperature relationship is opposite to that in the global soil dataset (Fig. 4b). This distinct behavior of MBT'$_{6Me}$ could be explained by the negative relationship between MAT and MAP in this region ($r^2 = 0.55$, $p < 0.01$; Fig. 1b) as opposed to their positive relationship globally. A similar relationship between MBT'$_{6Me}$ and MAT was found in an earlier study on arid temperate soils from northeastern China where MAT and MAP are also negatively correlated (Wang et al., 2016). Given the weak correlation between MAT and MBT'$_{5Me}$ ($r^2 = 0.19$, $p < 0.05$; Fig. 3o) and the strong correlation between MAT and MBT'$_{6Me}$ ($r^2 = 0.72$, $p < 0.01$; Fig. 3p) observed in this study, it may be worthwhile to also consider 6-methyl brGDGTs for MAT reconstructions in arid regions, where the MAT and MAP show a negative relationship.

Next to the high soil pH, the negative correlation between MAT and MAP/soil pH in this dataset ($r^2 = 0.55$, $p < 0.01$; Fig. 1b) may also contribute to the distinct response of 5- and 6-methyl brGDGTs to environmental changes, as these two parameters positively covary in the global soil dataset. The distinct behavior of 5- and 6-methyl brGDGTs agrees with the suggestion that they may be produced by different subdivisions within the phylum of Acidobacteria (Sinninghe Damsté et al., 2018), which are known to thrive under different pH ranges (Jones et al., 2009). Similarly, the change of brGDGT distributions in lakes strongly relates to the bacterial community shifts under different redox conditions (Weber et al., 2018; van Bree et al., 2020). This furthermore suggests that brGDGT distributions are (also) driven by changes in the bacterial community rather than by membrane adaptation, as was recently shown for brGDGTs across bacterial community thresholds in temperature (De Jonge et al., 2019) and pH (De Jonge et al., 2021). In addition, aridity has been shown to replace soil pH as main driver of the abundance and composition of the bacterial community in arid and semiarid grassland soils (Maestre et al., 2015; Neilson et al., 2017; Durán and Delgado-Baquerizo, 2020), and could thus exert a major influence on the distribution of brGDGTs in the Inner Mongolia transect.

3.2. *Comparison of soil bacterial community composition and brGDGT changes along the aridity transect*

In an attempt to inform on the possible producers of brGDGTs, changes in the soil bacterial community composition were compared with those in brGDGTs along the same soil transect. Liu et al. (2019) have previously described the bacterial diversity in the Inner Mongolia transect, which remains constant or increases with increasing aridity along the soil transect and shows that the soil bacterial community is dominated by 11 phyla, of which Actinobacteria (relative abundance 43.7 ± 7.4%, mean ± standard deviation), Proteobacteria (21.7 ± 4.1%), Acidobacteria (11.8 ± 4.8%), and Verrucomicrobia (5.1 ± 5.4%) are the most abundant. Of these phyla, Acidobacteria have been identified as a likely source of brGDGTs, as certain subdivisions are able to produce the building blocks (i.e. *iso*-diabolic acid) of 5- and 6-methyl brGDGTs (Sinninghe Damsté et al., 2011, 2014, 2018). Along the aridity transect, however, the relative abundance of Acidobacteria does not show a clear trend with soil pH or aridity (Fig. 5a,e). This may result from the high soil pH (> 7.5), as Acidobacteria generally prefer lower soil pH conditions (Sait et al., 2006; Jones et al., 2009). Only subdivision 4 (SD 4) appears relatively abundant in arid regions with high pH soils

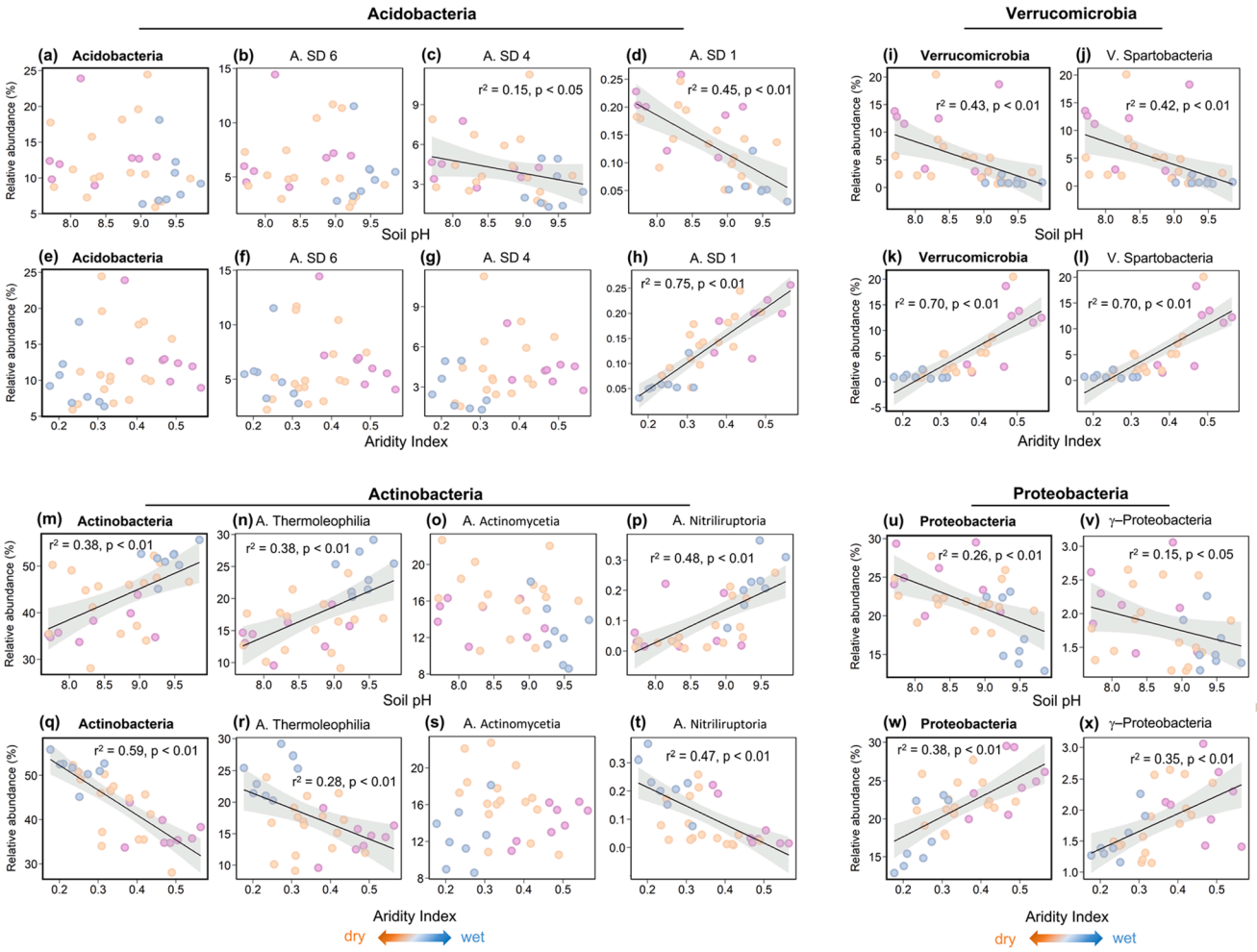

Fig. 5. Spearman's correlation of the bacterial community composition with soil pH and the aridity index (AI) for the phylum Acidobacteria (in bold) and the main subclasses SD 6, 4, and 1 (a–h), for the phylum Verrucomicrobia (in bold) and the main subclass Spartobacteria (i–l), and the phylum Actinobacteria (in bold) and the main subclasses Thermoleophilia, Actinomycetia, and Nitriliruptoria (m–t), and the phylum Proteobacteria (in bold) and the main subclass γ-Proteobacteria (u–x). The linear regression lines of correlations with $p < 0.05$ are plotted, the 95% confidence intervals are displayed by the gray shaded area.

(Jones et al., 2009; Fierer et al., 2012). Also the strains of SD 6, 7, and 16 positively relate with soil pH on a global scale, but they are generally less abundant than SD 4 (Jones et al., 2009).

Interestingly, SD 4 is the only subdivision that has so far been found to produce 5-methyl *iso*-diabolic acid and its methylated versions, whereas most of the SD 4 strains have been cultured from alkaline, dryland/savanna type soils (Janssen, 2006; Pankratov, 2012; Sinninghe Damsté et al., 2018). However, 5-methyl brGDGTs have the highest fractional abundance in more humid part of the Inner Mongolia soil transect, where MAT and soil pH are the lowest (Fig. 2). Also in the global soil dataset the 5-methyl brGDGTs are more abundant in acidic soils (De Jonge et al., 2014a), which is inconsistent with the warm and alkaline conditions from which SD 4 species have been isolated. De Jonge et al. (2021) hypothesized that SD 4 could be responsible for the production of 5-methyl brGDGTs with cyclopentane groups in mid- and high latitude soils. However, SD 4 does not show a clear trend with pH or aridity in Inner Mongolia (Fig. 5c,g), unlike the 5-methyl brGDGTs (Fig. 2). Of the cultured subdivisions that can produce 6-methyl *iso*-diabolic acid (i.e., SD 1, 3, and 6), only SD 6 increases with soil pH on a global scale (Jones et al., 2009; Fierer et al., 2012; Kielak et al., 2016; Sinninghe Damsté et al., 2018; De Jonge et al., 2021), but not in the Inner Mongolia soils, where it shows no response (Fig. 5b). Although it has been suggested that SD 6 responds to calcium content rather than soil pH (Navarrete et al., 2013; De Jonge et al., 2021), the relative abundance of SD 6 is not related to the calcium content in the Inner Mongolia soils ($r^2 = 0.01$, $p = 0.66$; Liu et al., 2019). SD 1 does relate with soil pH along the aridity transect ($r^2 = 0.45$, $p < 0.01$; Fig. 5d), although their abundance is very low compared to that of SD 4 and SD 6 risking overinterpretation of the trends. In addition, SD 1 has a negative relationship with soil pH, opposite to 6-methyl brGDGTs both in our aridity transect (Fig. 2) and in the global soil calibration set (De Jonge et al., 2014a).

The above result suggests that instead of Acidobacteria, other bacterial phyla could be the producers of brGDGTs in our transect. The relative abundances of the three other main phyla present in the transect does respond to soil pH and aridity (Fig. 5i,m,u), where aridity consistently explains most of the variation (Fig. 5k,q,w). Also the relationships of Actinobacteria, Proteobacteria, and Verrucomicrobia with aridity follow those established on a global scale (Maestre et al., 2015). Of these phyla, Verrucomicrobia show the strongest relationship with aridity ($r^2 = 0.70$, $p < 0.01$; Fig. 5k), which is mostly explained by Spartobacteria, the main subclass of Verrucomicrobia ($r^2 = 0.70$, $p < 0.01$; Fig. 5l), although its relationship with soil pH (Fig. 5j) is opposite to that observed in earlier studies on soils with pH < 7.5 (Shen et al., 2017; De Jonge et al., 2021).

Verrucomicrobia are aerobic heterotrophs and are ubiquitous and abundant in soils globally (Janssen, 2006), similar to the presumed heterotrophic lifestyle of brGDGT producers (Weijers et al., 2010), and follow the same trend as the 5-methyl brGDGTs (Fig. 2). Similar to Acidobacteria, Verrucomicrobia are able to thrive under low nutrient

conditions (Fierer et al., 2007, 2012), and occupy the same ecological niche in dryland soils, where they follow a fast-response life-strategy, for example, to wetting (Barnard et al., 2013). Although the membrane lipid composition, and thus the presence of brGDGT (precursor) lipids in this phylum has not (yet) been structurally investigated, the presence of *iso*-$C_{15:0}$ fatty acids, which are presumed building blocks for *iso*-diabolic acid (Sinninghe Damsté et al., 2011), has been reported for several Verrucomicrobia isolates. Specifically, *iso*-$C_{15:0}$ was found in Methylacidiphilae belonging to methanotrophic Verrucomicrobia isolated from geothermal habitats, with an optimum soil pH between 2 and 3.5, and optimum growth temperature around 55 °C (Dunfield et al., 2007; Op den Camp et al., 2009). The *iso*-$C_{15:0}$ was also reported as the major cellular fatty acids of three species belonging to the subclass Opitutae from the surface of a freshwater lake in Germany (Rast et al., 2017). Nevertheless, Verrucomicrobia strains isolated from soils so far seem to produce mainly *anteis*-$C_{15:0}$ and $C_{15:0}$, instead of *iso*-$C_{15:0}$ fatty acids (Sangwan et al., 2004; Otsuka et al., 2013), and the relative abundance of Methylacidiphilae and Opitutae is low (< 0.1%) along our soil transect.

Although a link between brGDGTs and Actinobacteria has not been reported before, the Actinobacteria, dominated by the subclass of Thermoleophilia in our aridity transect, is the only phylum that shows a strong positive relationship with aridity along the soil transect (r^2 = 0.59, $p < 0.01$; corresponding with a negative correlation with AI in Fig. 5q), similar to brGDGT-IIIa' (r^2 = 0.26, $p < 0.01$; Fig. 2). The presence of *iso*-$C_{15:0}$ fatty acids has been reported for members of the subclass Actinomycetia isolated from desert soils in Chile (Carro et al., 2019) and Egypt (Li et al., 2005), saline-alkaline soils in northwest China (Tang et al., 2008), and steppe soils in Russia (Nikitina et al., 2020) and Korea (Jin et al., 2013), most of which have an optimum pH of 7–9, a growth temperature of 28–30 °C and an aerobic lifestyle. Although Actinomycetia are abundant along our soil transect, they do not show a clear trend with soil pH or aridity (relative abundance = 9–23%, Fig. 5o,s). The *iso*-$C_{15:0}$ was also detected in members of the subclass Nitriliruptoria that were isolated from saline-alkaline soils in northwest China (Zhang et al., 2016). The Nitriliruptoria show a positive relationship with aridity along the aridity transect ($r^2 = 0.47$, $p < 0.01$; Fig. 5t), consistent with that of brGDGT-IIIa'. Finally, γ-Proteobacteria also show the same trend with aridity as 5-methyl brGDGTs ($r^2 = 0.35$, $p < 0.01$; Fig. 5x), and host species that produce *iso*-$C_{15:0}$ fatty acids (Jung et al., 2009; Kim et al., 2014; Fang et al., 2015). Despite the shared trends along the transect, it remains challenging to identify the specific producer of brGDGTs by simply comparing the bacterial community composition with the trends in brGDGTs along this aridity transect. For example, trends observed here may be influenced by differences in the preservation potential of DNA and brGDGTs, and the fact that some of the cultured species make one of the presumed brGDGT building blocks does not yet guarantee that they also produce brGDGTs. Nevertheless, Verrucomicrobia and Actinobacteria could be further investigated as (one of the) possible producer of 5- and 6-methyl brGDGTs in arid soils, respectively.

4. Conclusions

The combined analysis of brGDGTs and the soil bacterial community composition in soils along an aridity transect in Inner Mongolia reveals that 5-methyl and 6-methyl brGDGT isomers respond differently to aridity and associated changes in soil pH. Whereas the isomer ratio positively correlates with aridity and soil pH, following global trends, the degree of cyclization no longer responds in soils with pH > 7.5. Only the $\#rings_{penta}$ displays relatively weak, but notably opposite trend with aridity and soil pH when determined for either 5- or 6-methyl brGDGTs. This implies that the use of a transfer function based on the relative abundance of 6-methyl brGDGTs is recommended to reduce uncertainties on brGDGT-based reconstructed soil pH. Similarly, the degree of methylation of 5- and 6-methyl brGDGTs have opposite relationships with MAT along the transect. The distinct responses of 5- and 6-methyl brGDGTs to environmental changes indicate that they are more likely driven by shifts in the soil bacterial communities instead of by biophysiological adjustments of their membrane structures. Although opposite to that in the global soil dataset, the strong relationship between MBT'_{6Me} and MAT indicates that the MBT'_{6Me} is worth being considered for temperature reconstructions in arid regions with high soil pH and where the MAT and MAP are negatively correlated. Finally, comparison of brGDGT signals with changes in the bacterial community composition in the same soil transect reveals that Acidobacteria are not likely the main producers of brGDGTs in this transect. Instead, Verrucomicrobia and Actinobacteria share the same response to aridity as 5- and 6-methyl brGDGTs, respectively. Based on the fact that some Verrucomicrobia and Actinobacteria isolates contain *iso*-$C_{15:0}$ fatty acids, we propose that Verrucomicrobia and Actinobacteria could be a potential candidate to produce (a)cyclic 5- and 6-methyl brGDGTs in alkaline soils from arid regions, which deserves future investigation.

Declaration of Competing Interest

The authors declare that they have no known competing financial interests or personal relationships that could have appeared to influence the work reported in this paper.

Data availability statement

All data can be found online and in PANGEA (https://doi.org/10.1594/PANGAEA.938067).

Acknowledgements

We thank Klaas Nierop for laboratory assistance at Utrecht University. The editors, Cindy De Jonge, and an anonymous reviewer are appreciated for their feedback that has further improved this manuscript. This project received funding from the China Exchange Program of the Royal Netherlands Academy of Arts and Sciences (KNAW, grant no. 530-6CDP17 to XF and FP), and the Dutch Research Council (NWO, Vidi grant no. 192.071 to FP).

Appendix A. Supplementary material

Supplementary data to this article can be found online at https://doi.org/10.1016/j.orggeochem.2021.104347.

References

Barnard, R.L., Osborne, C.A., Firestone, M.K., 2013. Responses of soil bacterial and fungal communities to extreme desiccation and rewetting. ISME Journal 7, 2229–2241.

Bligh, E.G., Dyer, W.J., 1959. A rapid method of total lipid extraction and purification. Canadian Journal of Biochemistry and Physiology 37, 911–917.

Carro, L., Golinska, P., Nouioui, I., Bull, A.T., Igual, J.M., Andrews, B.A., Klenk, H.P., Goodfellow, M., 2019. *Micromonospora acroterricola* sp. nov., a novel actinobacterium isolated from a high altitude atacama desert soil. International Journal of Systematic and Evolutionary Microbiology 69, 3426–3436.

Chen, C., Bai, Y., Fang, X., Zhuang, G., Khodzhiev, A., Bai, X., Murodov, A., 2021. Evaluating the potential of soil bacterial tetraether proxies in westerlies dominating western Pamirs, Tajikistan and implications for paleoenvironmental reconstructions. Chemical Geology 559, 119908. https://doi.org/10.1016/j.chemgeo.2020.119908.

Dang, X., Yang, H., Naafs, B.D.A., Pancost, R.D., Xie, S., 2016. Evidence of moisture control on the methylation of branched glycerol dialkyl glycerol tetraethers in semi-arid and arid soils. Geochimica et Cosmochimica Acta 189, 24–36.

De Jonge, C., Hopmans, E.C., Stadnitskaia, A., Rijpstra, W.I.C., Hofland, R., Tegelaar, E., Sinninghe Damsté, J.S., 2013. Identification of novel penta- and hexamethylated branched glycerol dialkyl glycerol tetraethers in peat using HPLC–MS^2, GC–MS and GC–SMB-MS. Organic Geochemistry 54, 78–82.

De Jonge, C., Hopmans, E.C., Zell, C.I., Kim, J.-H., Schouten, S., Sinninghe Damsté, J.S., 2014a. Occurrence and abundance of 6-methyl branched glycerol dialkyl glycerol tetraethers in soils: Implications for palaeoclimate reconstruction. Geochimica et Cosmochimica Acta 141, 97–112.

De Jonge, C., Stadnitskaia, A., Hopmans, E.C., Cherkashov, G., Fedotov, A., Sinninghe Damsté, J.S., 2014b. In situ produced branched glycerol dialkyl glycerol tetraethers

in suspended particulate matter from the Yenisei River, Eastern Siberia. Geochimica et Cosmochimica Acta 125, 476–491.
De Jonge, C., Radujković, D., Sigurdsson, B.D., Weedon, J.T., Janssens, I., Peterse, F., 2019. Lipid biomarker temperature proxy responds to abrupt shift in the bacterial community composition in geothermally heated soils. Organic Geochemistry 137, 103897. https://doi.org/10.1016/j.orggeochem.2019.07.006.
De Jonge, C., Kuramae, E.E., Radujković, D., Weedon, J.T., Janssens, I.A., Peterse, F., 2021. The influence of soil chemistry on branched tetraether lipids in mid- and high latitude soils: Implications for brGDGT-based paleothermometry. Geochimica et Cosmochimica Acta 310, 95–112.
Dearing Crampton-Flood, E., Tierney, J.E., Peterse, F., Kirkels, F.M.S.A., Sinninghe Damsté, J.S., 2020. BayMBT: A Bayesian calibration model for branched glycerol dialkyl glycerol tetraethers in soils and peats. Geochimica et Cosmochimica Acta 268, 142–159.
Ding, S., Schwab, V.F., Ueberschaar, N., Roth, V.-N., Lange, M., Xu, Y., Gleixner, G., Pohnert, G., 2016. Identification of novel 7-methyl and cyclopentanyl branched glycerol dialkyl glycerol tetraethers in lake sediments. Organic Geochemistry 102, 52–58.
Ding, S., Xu, Y., Wang, Y., He, Y., Hou, J., Chen, L., He, J.-S., 2015. Distribution of branched glycerol dialkyl glycerol tetraethers in surface soils of the Qinghai-Tibetan Plateau: Implications of brGDGTs-based proxies in cold and dry regions. Biogeosciences 12 (11), 3141–3151.
Dirghangi, S.S., Pagani, M., Hren, M.T., Tipple, B.J., 2013. Distribution of glycerol dialkyl glycerol tetraethers in soils from two environmental transects in the USA. Organic Geochemistry 59, 49–60.
Dunfield, P.F., Yuryev, A., Senin, P., Smirnova, A.V., Stott, M.B., Hou, S., Ly, B., Saw, J. H., Zhou, Z., Ren, Y., Wang, J., Mountain, B.W., Crowe, M.A., Weatherby, T.M., Bodelier, P.L.E., Liesack, W., Feng, L.u., Wang, L., Alam, M., 2007. Methane oxidation by an extremely acidophilic bacterium of the phylum Verrucomicrobia. Nature 450, 879–882.
Durán, J., Delgado-Baquerizo, M., 2020. Vegetation structure determines the spatial variability of soil biodiversity across biomes. Scientific Reports 10, 1–7.
Fang, T., Wang, H., Huang, Y., Zhou, H., Dong, P., 2015. *Oleiagrimonas soli* gen. nov., sp. nov., a genome-sequenced gammaproteobacterium isolated from an oilfield. International Journal of Systematic and Evolutionary Microbiology 65, 1666–1671.
Fierer, N., Bradford, M.A., Jackson, R.B., 2007. Toward an ecological classification of soil bacteria. Ecology 88, 1354–1364.
Fierer, N., Leff, J.W., Adams, B.J., Nielsen, U.N., Bates, S.T., Lauber, C.L., Owens, S., Gilbert, J.A., Wall, D.H., Caporaso, J.G., 2012. Cross-biome metagenomic analyses of soil microbial communities and their functional attributes. Proceedings of the National Academy of Sciences 109, 21390–21395.
Hopmans, E.C., Schouten, S., Sinninghe Damsté, J.S., 2016. The effect of improved chromatography on GDGT-based palaeoproxies. Organic Geochemistry 93, 1–6.
Huguet, C., Hopmans, E.C., Febo-Ayala, W., Thompson, D.H., Sinninghe Damsté, J.S., Schouten, S., 2006. An improved method to determine the absolute abundance of glycerol dibiphytanyl glycerol tetraether lipids. Organic Geochemistry 37, 1036–1041.
IUSS Working Group WRB, 2015. World Reference Base for Soil Resources 2014, update 2015. International soil classification system for naming soils and creating legends for soil maps. World Soil Resources Reports No. 106. FAO, Rome.
Janssen, P.H., 2006. Identifying the dominant soil bacterial taxa in libraries of 16S rRNA and 16S rRNA genes. Applied and Environmental Microbiology 72, 1719–1728.
Jin, L., Lee, H.G., Kim, H.S., Ahn, C.Y., Oh, H.M., 2013. *Geodermatophilus soli* sp. nov. and *Geodermatophilus terrae* sp. nov., two actinobacteria isolated from grass soil. International Journal of Systematic and Evolutionary Microbiology 63, 2625–2629.
Jones, R.T., Robeson, M.S., Lauber, C.L., Hamady, M., Knight, R., Fierer, N., 2009. A comprehensive survey of soil acidobacterial diversity using pyrosequencing and clone library analyses. ISME Journal 3, 442–453.
Jung, H.-M., Ten, L.N., Kim, K.-H., An, D.S., Im, W.-T., Lee, S.-T., 2009. *Dyella ginsengisoli* sp. nov., isolated from soil of a ginseng field in South Korea. International Journal of Systematic and Evolutionary Microbiology 59, 460–465.
Kielak, A.M., Barreto, C.C., Kowalchuk, G.A., van Veen, J.A., Kuramae, E.E., 2016. The ecology of Acidobacteria: Moving beyond genes and genomes. Frontiers in Microbiology 7, 1–16.
Kim, M.-S., Hyun, D.-W., Kim, J.Y., Kim, S., Bae, J.-W., Park, E.-J., 2014. *Dyella jejuensis* sp. nov., isolated from soil of Hallasan Mountain in Jeju Island. Journal of Microbiology 52, 373–377.
Li, W.J., Chen, H.H., Zhang, Y.Q., Kim, C.J., Park, D.J., Lee, J.C., Xu, L.H., Jiang, C.L., 2005. *Citricoccus alkalitolerans* sp. nov., a novel actinobacterium isolated from a desert soil in Egypt. International Journal of Systematic and Evolutionary Microbiology 55, 87–90.
Liu, N., Hu, H., Ma, W., Deng, Y., Liu, Y., Hao, B., Zhang, X., Dimitrov, D., Feng, X., Wang, Z., 2019. Contrasting biogeographic patterns of bacterial and archaeal diversity in the top- and subsoils of temperate grasslands. mSystems 4, 1–18.
Maestre, F.T., Delgado-Baquerizo, M., Jeffries, T.C., Eldridge, D.J., Ochoa, V., Gozalo, B., Quero, J.L., García-Gómez, M., Gallardo, A., Ulrich, W., Bowker, M.A., Arredondo, T., Barraza-Zepeda, C., Bran, D., Florentino, A., Gaitán, J., Gutiérrez, J. R., Huber-Sannwald, E., Jankju, M., Mau, R.L., Miriti, M., Naseri, K., Ospina, A., Stavi, I., Wang, D., Woods, N.N., Yuan, X., Zaady, E., Singh, B.K., 2015. Increasing aridity reduces soil microbial diversity and abundance in global drylands. Proceedings of the National Academy of Sciences 112, 15684–15689.
Menges, J., Huguet, C., Alcañiz, J.M., Fietz, S., Sachse, D., Rosell-Melé, A., 2014. Influence of water availability in the distributions of branched glycerol dialkyl glycerol tetraether in soils of the Iberian Peninsula. Biogeosciences 11, 2571–2581.
Naafs, B.D.A., Gallego-Sala, A.V., Inglis, G.N., Pancost, R.D., 2017. Refining the global branched glycerol dialkyl glycerol tetraether (brGDGT) soil temperature calibration. Organic Geochemistry 106, 48–56.
Naafs, B.D.A., Oliveira, A.S.F., Mulholland, A.J., 2021. Molecular dynamics simulations support the hypothesis that the brGDGT paleothermometer is based on homeoviscous adaptation. Geochimica et Cosmochimica Acta 312, 44–56.
Navarrete, A.A., Kuramae, E.E., de Hollander, M., Pijl, A.S., van Veen, J.A., Tsai, S.M., 2013. Acidobacterial community responses to agricultural management of soybean in Amazon forest soils. FEMS Microbiology Ecology 83, 607–621.
Neilson, J.W., Califf, K., Cardona, C., Copeland, A., van Treuren, W., Josephson, K.L., Knight, R., Gilbert, J.A., Quade, J., Caporaso, J.G., Maier, R.M., 2017. Significant impacts of increasing aridity on the arid soil microbiome. mSystems 2, 1–15.
Nikitina, E., Liu, S.W., Li, F.N., Buyantueva, L., Abidueva, E., Sun, C.H., 2020. *Glycomyces buryatensis* sp. nov., an actinobacterium isolated from steppe soil. International Journal of Systematic and Evolutionary Microbiology 70, 1356–1363.
Op den Camp, H.J.M., Islam, T., Stott, M.B., Harhangi, H.R., Hynes, A., Schouten, S., Jetten, M.S.M., Birkeland, N.K., Pol, A., Dunfield, P.F., 2009. Environmental, genomic and taxonomic perspectives on methanotrophic Verrucomicrobia. Environmental Microbiology Reports 1, 293–306.
Otsuka, S., Ueda, H., Suenaga, T., Uchino, Y., Hamada, M., Yokota, A., Senoo, K., 2013. *Roseimicrobium gellanilyticum* gen. nov., sp. nov., a new member of the class Verrucomicrobiae. International Journal of Systematic and Evolutionary Microbiology 63, 1982–1986.
Pankratov, T.A., 2012. Acidobacteria in microbial communities of the bog and tundra lichens. Microbiology 81, 51–58.
Peterse, F., van der Meer, J., Schouten, S., Weijers, J.W.H., Fierer, N., Jackson, R.B., Kim, J.H., Sinninghe Damsté, J.S., 2012. Revised calibration of the MBT-CBT paleotemperature proxy based on branched tetraether membrane lipids in surface soils. Geochimica et Cosmochimica Acta 96, 215–229.
R Core Team: R: A language and environment for statistical computing. R Foundation for Statistical Computing, Vienna, Austria, available at: http://www.R-project.org, last access: March 2021.
Rast, P., Glöckner, I., Boedeker, C., Jeske, O., Wiegand, S., Reinhardt, R., Schumann, P., Rohde, M., Spring, S., Glöckner, F.O., Jogler, C., Jogler, M., 2017. Three novel species with peptidoglycan cell walls form the new genus *Lacunisphaera* gen. nov. in the family opitutaceae of the verrucomicrobial subdivision 4. Frontiers in Microbiology 8, 1–18.
Sait, M., Davis, K.E.R., Janssen, P.H., 2006. Effect of pH on isolation and distribution of members of subdivision 1 of the phylum *Acidobacteria* occurring in soil. Applied and Environmental Microbiology 72, 1852–1857.
Sangwan, P., Chen, X., Hugenholtz, P., Janssen, P.H., 2004. *Chthoniobacter flavus* gen. nov., sp. nov., the first pure-culture representative of subdivision two, *Spartobacteria classis* nov., of the phylum *Verrucomicrobia*. Applied and Environmental Microbiology 70, 5875–5881.
Schouten, S., Hopmans, E.C., Sinninghe Damsté, J.S., 2013. The organic geochemistry of glycerol dialkyl glycerol tetraether lipids: A review. Orgaic Geochemistry 54, 19–61.
Shen, C., Ge, Y., Yang, T., Chu, H., 2017. Verrucomicrobial elevational distribution was strongly influenced by soil pH and carbon/nitrogen ratio. Journal of Soils and Sediments 17, 2449–2456.
Sinninghe Damsté, J.S., 2016. Spatial heterogeneity of sources of branched tetraethers in shelf systems: The geochemistry of tetraethers in the Berau River delta (Kalimantan, Indonesia). Geochimica et Cosmochimica Acta 186, 13–31.
Sinninghe Damsté, J.S., Hopmans, E.C., Pancost, R.D., Schouten, S., Geenevasen, J.A.J., 2000. Newly discovered non-isoprenoid glycerol dialkyl glycerol tetraether lipids in sediments. Chemical Communications 1683–1684.
Sinninghe Damsté, J.S., Rijpstra, W.I.C., Hopmans, E.C., Weijers, J.W.H., Foesel, B.U., Overmann, J., Dedysh, S.N., 2011. 13,16-Dimethyl octacosanedioic acid (*iso*-diabolic acid), a common membrane-spanning lipid of *Acidobacteria* subdivisions 1 and 3. Applied and Environmental Microbiology 77, 4147–4154.
Sinninghe Damsté, J.S., Rijpstra, W.I.C., Hopmans, E.C., Foesel, B.U., Wüst, P.K., Overmann, J., Tank, M., Bryant, D.A., Dunfield, P.F., Houghton, K., Stott, M.B., 2014. Ether- and ester-bound *iso*-diabolic acid and other lipids in members of *Acidobacteria* subdivision 4. Applied and Environmental Microbiology 80, 5207–5218.
Sinninghe Damsté, J.S., Rijpstra, W.I.C., Foesel, B.U., Huber, K.J., Overmann, J., Nakagawa, S., Kim, J.J., Dunfield, P.F., Dedysh, S.N., Villanueva, L., 2018. An overview of the occurrence of ether- and ester-linked iso-diabolic acid membrane lipids in microbial cultures of the Acidobacteria: Implications for brGDGT paleoproxies for temperature and pH. Organic Geochemistry 124, 63–76.
Tang, S.K., Wang, Y., Schumann, P., Stackebrandt, E., Lou, K., Jiang, C.L., Xu, L.H., Li, W. J., 2008. *Brevibacterium album* sp. nov., a novel actinobacterium isolated from a saline soil in China. International Journal of Systematic and Evolutionary Microbiology 58, 574–577.
van Bree, L.G.J., Peterse, F., Baxter, A.J., De Crop, W., van Grinsven, S., Villanueva, L., Verschuren, D., Sinninghe Damsté, J.S., 2020. Seasonal variability and sources of in situ brGDGT production in a permanently stratified African crater lake. Biogeosciences 17, 5443–5463.

van der Veen, I., Peterse, F., Davenport, J., Meese, B., Bookhagen, B., France-Lanord, C., Kahmen, A., Hassenruck-Gudipati, H.J., Gajurel, A., Strecker, M.R., Sachse, D., 2020. Validation and calibration of soil δ^2H and brGDGTs along (E-W) and strike (N-S) of the Himalayan climatic gradient. Geochimica et Cosmochimica Acta 290, 408–423.

Wang, H., Liu, W., Lu, H., 2016. Appraisal of branched glycerol dialkyl glycerol tetraether-based indices for North China. Organic Geochemistry 98, 118–130.

Wang, H., Liu, W., Zhang, C.L., 2014. Dependence of the cyclization of branched tetraethers on soil moisture in alkaline soils from arid-subhumid China: Implications for palaeorainfall reconstructions on the Chinese Loess Plateau. Biogeosciences 11, 6755–6768.

Weber, Y., Sinninghe Damsté, J.S., Zopfi, J., De Jonge, C., Gilli, A., Schubert, C.J., Lepori, F., Lehmann, M.F., Niemann, H., 2018. Redox-dependent niche differentiation provides evidence for multiple bacterial sources of glycerol tetraether lipids in lakes. Proceedings of the National Academy of Sciences 115, 10926–10931.

Weijers, J.W.H., Schouten, S., Hopmans, E.C., Geenevasen, J.A.J., David, O.R.P., Coleman, J.M., Pancost, R.D., Sinninghe Damsté, J.S., 2006. Membrane lipids of mesophilic anaerobic bacteria thriving in peats have typical archaeal traits. Environmental Microbiology 8, 648–657.

Weijers, J.W.H., Schouten, S., van den Donker, J.C., Hopmans, E.C., Sinninghe Damsté, J. S., 2007. Environmental controls on bacterial tetraether membrane lipid distribution in soils. Geochimica et Cosmochimica Acta 71, 703–713.

Weijers, J.W.H., Panoto, E., van bleijswijk, J., Schouten, S., Rijpstra, W.I.C., Balk, M., Stams, A.J.M., Sinninghe Damsté, J.S., 2009. Constraints on the biological source(s) of the orphan branched tetraether membrane lipids. Geomicrobiology Journal 26, 402–414.

Weijers, J.W.H., Wiesenberg, G.L.B., Bol, R., Hopmans, E.C., Pancost, R.D., 2010. Carbon isotopic composition of branched tetraether membrane lipids in soils suggest a rapid turnover and a heterotrophic life style of their source organism(s). Biogeosciences 7, 2959–2973.

Xie, S., Pancost, R.D., Chen, L., Evershed, R.P., Yang, H., Zhang, K., Huang, J., Xu, Y., 2012. Microbial lipid records of highly alkaline deposits and enhanced aridity associated with significant uplift of the Tibetan Plateau in the Late Miocene. Geology 40, 291–294.

Yang, H., Pancost, R.D., Dang, X., Zhou, X., Evershed, R.P., Xiao, G., Tang, C., Gao, L., Guo, Z., Xie, S., 2014. Correlations between microbial tetraether lipids and environmental variables in Chinese soils: Optimizing the paleo-reconstructions in semi-arid and arid regions. Geochimica et Cosmochimica Acta 126, 49–69.

Zhang, X., Dai, G., Ma, T., Liu, N., Hu, H., Ma, W., Zhang, J.-B., Wang, Z., Peterse, F., Feng, X., 2020. Links between microbial biomass and necromass components in the top- and subsoils of temperate grasslands along an aridity gradient. Geoderma 379, 114623.

Zhang, Y.G., Chen, J.Y., Wang, H.F., Xiao, M., Yang, L.L., Guo, J.W., Zhou, E.M., Zhang, Y.M., Li, W.J., 2016. *Egicoccus halophilus* gen. nov., sp. nov., a halophilic, alkalitolerant actinobacterium and proposal of *Egicoccaceae* fam. nov. and *Egicoccales* ord. nov. International Journal of Systematic and Evolutionary Microbiology 66, 530–535.